Accepted Manuscript

Constraining timing and tectonic implications of Neoproterozoic metamorphic event in the Cathaysia Block, South China

Jinlong Yao, Liangshu Shu, Peter A. Cawood, Jinyi Li

PII: S0301-9268(16)30260-1
DOI: http://dx.doi.org/10.1016/j.precamres.2017.01.032
Reference: PRECAM 4671

To appear in: *Precambrian Research*

Received Date: 13 July 2016
Revised Date: 22 October 2016
Accepted Date: 23 January 2017

Please cite this article as: J. Yao, L. Shu, P.A. Cawood, J. Li, Constraining timing and tectonic implications of Neoproterozoic metamorphic event in the Cathaysia Block, South China, *Precambrian Research* (2017), doi: http://dx.doi.org/10.1016/j.precamres.2017.01.032

Constraining timing and tectonic implications of Neoproterozoic metamorphic event in the Cathaysia Block, South China

Jinlong Yao[a], Liangshu Shu[a,*,Lsshu@nju.edu.cn], Peter A. Cawood[b, c], Jinyi Li[d]

[a] State Key Laboratory for Mineral Deposits Research, School of Earth Sciences and Engineering, Nanjing University, Nanjing 210093, China

[b] Department of Earth Sciences, University of St Andrews, North Street, St Andrews KY16 9AL, UK

[c] School of Earth, Atmosphere & Environment, Monash University, Melbourne, VIC 3800, Australia [d] Institute of Geology, Chinese Academy of Geological Sciences, Beijing 100037, China

* Corresponding author E–mail: Lsshu@nju.edu.cn

Abstract

The Cathaysia Block of the South China Craton includes a Proterozoic basement that experienced a prolonged Precambrian crustal evolution but to date lacks evidence of Proterozoic metamorphic ages. At Lichuan and Jianning, in the Wuyi Domain of the eastern Cathaysia Block, Proterozoic rock units include migmatized paragneiss of the Wanyuan Group and minor amphibolite of the Tianjingping Formation, which are enveloped by schist of Mayuan Group, and all are intruded by Paleozoic and Mesozoic igneous rocks. Detrital zircon grains from the Wanyuan paragneiss display metamorphic rims that yield concordant weighted average $^{206}Pb/^{238}U$ ages of 860 ± 6

Ma and 435 ± 5 Ma, along with variably disconcordant ages with lower intercept ages of 442 ± 41 Ma. The zircon core ages range from 3015 Ma to 851 Ma, with three major age populations at 930–865 Ma, 1850–1200 Ma and 2650–2400 Ma. Detrital zircon grains from Mayuan schist samples at Jianning generally lack core-rim structures and yield three main age populations at 860–736 Ma, 1835–1775 Ma and 2720–2500 Ma. Metamorphic ages of ca. 860 Ma and ca. 435 Ma for the Wanyuan paragneiss along with the youngest detrital zircon constrain the depositional age of the protolith to ca. 865–860 Ma, whereas the Mayuan Group is younger and probably deposited after ca. 736 Ma. Characteristics of detrital zircon age populations along with regional geological data suggest accumulation of the Wanyuan Group in a convergent and/or collisional setting. Metamorphism and a possible subduction -collision process within the Cathaysia Block at around 860 Ma suggest it was not a unified block in early Neoproterozoic. The growth of ca. 440 Ma metamorphic rims is likely related to granitic magmatism, such as that exposed in the Lichuan region. The sparse evidence for early Neoproterozoic metamorphism likely reflects widespread overprinting by the Paleozoic tectonothermal event at around 440 Ma.

Keywords: Detrital zircon; Geochronology; Paragneiss; early Neoproterozoic metamorphism, Cathaysia Block, South China

1. Introduction

Regional metamorphism and tectonothermal events associated with orogenesis are generally ascribed to subduction or collision zone settings and their timing provides important constraints on the crustal evolution of the resultant mountain belts.

In regions that have undergone multiple metamorphic events, recognition of the earliest events and their tectonic setting can be difficult to determine due to overprinting by younger events including the resetting of mineral systems. Advances in micro-analysis along with the stability of the U–Th–Pb isotopic system in zircon and its ability to record multiple igneous and metamorphic events have made it an important phase in unravelling complex geological histories in orogenic belts (Vavra et al., 1999; Corfu et al., 2003; Harley et al., 2007).

The Cathaysia Block of the southeast South China Craton contains the geographically restricted Paleoproterozoic Wuyi domain, and the early Neoproterozoic Yunkai and Southern Jiangxi – Nanling domains, overlain by widespread middle Neoproterozoic to early Paleozoic sedimentary and igneous units (Fig. 1; Shu, 2006; Zhao and Cawood, 1999, 2012; Li et al., 2011a, b; Wang et al., 2014). Early Neoproterozoic subduction related igneous suites (Shu et al. 2008; Li et al., 2011b; Zhang et al., 2012; Wang et al., 2013) and S type granitic gneiss (Wang et al., 2014) are exposed in various localities of the Cathaysia Block. Due to a lack of evidence of Neoproterozoic metamorphism, whether the Cathaysia Block constituted a single unified block or a series of micro-blocks assembled in the Neoproterozoic is debated, as is the number and direction of subduction zones, and the timing of final suturing with the Yangtze Block (Shu, 2012; Wang et al., 2013, 2014; Yao et al., 2014, 2015; Zhao et al., 2015). These uncertainties are reflected in the controversy as to the position of South China in the Rodinia supercontinent (Cawood et al., 2013; Wang et al., 2013).

In this study, we outline U-Pb zircon age data from migmatized paragneiss from the Cathaysia Block of the South China Craton, which provide the unequivocal age data for early Neoproterozoic metamorphism of the block. The studied rock units preserve a spectrum of detrital zircon ages that are variably overprinted by early Neoproterozoic and early Paleozoic metamorphic events, providing insight into the assembly of the Cathaysia Block that we relate to subduction-collision related tectono-thermal events.

2. Geological setting and litho-stratigraphic structures

2.1. Geological setting

The Cathaysia Block accreted with the Yangtze Block to the northwest in the early-middle Neoproterozoic, involving a series of arc systems along the intervening Jiangnan accretionary orogenic belt (Cawood et al.., 2013 and references therein; Yao et al., 2015, 2016). These are overlain by Nanhua rift basin succession and Sinian to Phanerozoic strata (Shu et al., 2011; Shu, 2012).

In the period ca. 440–410 Ma, the pre-Devonian (> ca. 410 Ma) rock units in Cathaysia were variably metamorphosed and deformed, and intruded by S-type granites (Charvet et al., 2010; Shu et al., 2014; Song et al., 2015). Coeval metamorphism of early Paleozoic strata reached greenschist facies in the Cathaysia Block, and locally amphibolite to granulite facies (BGMRFJ, 1985; Zhao and Cawood, 1999; Yu et al. 2003, 2005), but the precise age of metamorphism is not well constrained. Zhao and Cawood (1999) identified four stages of metamorphism from the Mayuan Group in Wuyi Domain that display a clockwise P-T path. The Yangtze Block generally lacks evidence for an early Paleozoic tectonothermal event (Fig. 1; Shu, 2012; Zhao and Cawood, 2012).

2.2. Lithology and related structures in Lichuan and Jianning regions

In the Lichuan region of the western Wuyi Domain, the Wanyuan Group is the oldest exposed unit and is unconformably overlain by the middle to late Neoproterozoic Sinian Group (Fig. 2; BGMRJX, 1984). The former consists of variably migmatized gneiss and leptynite pods or lenses interlayered within schist and minor amphibolite (BGMRJX, 1984). The Sinian Group contains variably migmatized mica schist and phyllite. Both the Wanyuan and Sinian groups are intruded by deformed S-type granite dated at 436 ± 6 Ma and 457 ± 6 Ma (LA–ICP–MS, Zhang et al., 2011; Song et al., 2015 and references therein) and undeformed Mesozoic plutons dated at 189 ± 5 Ma (LA–ICP–MS, Jiang et al., 2015). Exposures of paragneiss and migmatized paragneiss ranging in size from tens of centimeters to kilometers occur within the Paleozoic granitic plutons (Fig. 2, 3a).

To the south of Lichuan, at Jianning, plagioclase amphibolite of the Tianjingping Formation is enveloped by kyanite schist and biotite quartz schist of the Mayuan Group (BGMRFJ, 1985; Fig. 2, 4). The Tianjingping Formation is dated at 1766 ± 19 Ma (zircon SHRIMP U–Pb, Li, 1997) and the Mayuan Group is likely Neoproterozoic (Wan et al., 2007). Both units have experienced multiple episodes of deformation and metamorphism (Fig. 3b; Zhao and Cawood, 1999) and are intruded by Paleozoic

S-type granite dated at 438 ± 7 Ma (Zhang et al., 2011) and diorite and Mesozoic S-type granite (Fig. 3). Electron microprobe (EMP) ages on monazite from mica quartz schist of the Mayuan Group in the Jianning area yielded an age of 443 ± 11 Ma (Chen et al., 2008), and are similar to ages of 446-425 Ma reported on metamorphic rims developed on detrital zircons within the group (Wan et al., 2007).

2.3. Sample descriptions

Sample locations are shown on figures 2 and 3. They include three migmatized paragneisses (1523, 1523–1 and 1523–2; GPS: N27°17.363', E116°54.081') (Fig. 4), assigned to the Wanyuan Group, which are engulfed by Paleozoic gneissic S-type granite in the Lichuan area, and three schists 1515 (GPS: N26°56.978', E116°41.665') (Fig. 4), 1519 (GPS: N26°56.758', E116°42.298') and 1521 (GPS: N26°52.451', E116°42.771') from the Mayuan Group in the Jianning area. The leucosome and melanosome of the migmatized paragneisses from Lichuan were not separated during sample preparation.

The migmatized paragneiss samples 1523 and 1523–1 contain about 42% altered plagioclase, 20% quartz, 22% biotite, 8% hornblende and 8% garnet (Fig. 5), whereas biotite gneiss sample 1523–2 contains 45% plagioclase, 30% quartz, 20% hornblende and 5% garnet (Fig. 5). Biotite quartz schist sample 1517 contains 60% quartz, 25% biotite, 5% plagioclase and 10% sericite and chlorite, whereas kyanite biotite quartz schist sample 1519 has 45% quartz, 25% biotite, 15% plagioclase and 15% kyanite. The other kyanite schist, sample 1521, contains about 35% kyanite, 45% quartz, 15% plagioclase and 5% calcite (Fig. 5).

ACCEPTED MANUSCRIPT

3. Analytical procedures

Zircons were separated from the crushed rocks using heavy liquid and magnetic techniques and then handpicked under a binocular microscope. The zircon grains were mounted in epoxy resin, polished and coated. Cathodoluminescence (CL) images of the zircons were obtained using a Quanta 400 FEG electron microscope equipped with Mono CL3+ (Gatan, U.S.A.) at the State Key Laboratory of Continental Dynamics in Northwest University.

Zircon U–Pb isotopic dating was carried out at the State Key Laboratory for Mineral Deposits Research in Nanjing University, using an Agilent 7500a ICP–MS connected to a New Wave 213 nm laser ablation system. The U–Pb fractionation was corrected using zircon standard GEMOC GJ–1 with an age of 601 ± 12 Ma and accuracy was controlled by using the zircon standard Mud Tank with an age of 735 ± 12 Ma. The U–Pb ages were calculated from the original signal data using the Glitter software and U–Th–Pb age data are plotted on concordia diagrams using the Isoplot program (Ludwig, 2003). Zircons older than 1000 Ma have high contents of radiogenic Pb, hence $^{207}Pb/^{206}Pb$ age is more reliable and used to determine the crystallization age. On the other hand, due to low content of radiogenic Pb, the $^{206}Pb/^{238}U$ age is more reliable for zircons with ages younger than 1000 Ma.

4. Analytical results

More than 90 % of the zircons from migmatized paragneiss samples (1523 and 1523–1) display core-rim structures with the cores mostly of magmatic origin and rims being highly luminescent with no oscillatory zone and are inferred to be of metamorphic origin (Fig. 6), consistent with their lower Th/U ratios, though Th/U ratio is not an exclusive indicator of zircon origins. Zircon grains obtained from the migmatized gneiss samples show varied morphology, most are angular but with a minor component displaying a rounded morphology.

A total of 57 analysis were conducted on cores and rims of grains from migmatized paragneiss sample 1523 and yielded ages ranging from 3015 Ma to 421 Ma (Fig. 7). Seven analyses on metamorphic rims yield concordant ages with a weighted average $^{206}Pb/^{238}U$ age of 860 ± 8 Ma (MSWD = 0.19, n = 7) (Fig. 8), whereas another 23 analysis on metamorphic rims were variably discordant with a lower intercept age of 424 ± 39 Ma (MSWD = 26, n = 23). Four of the ages were concordant between 442–427 Ma and with a weighted average $^{206}Pb/^{238}U$ age of 434 ± 6 Ma (MSWD = 0.87) (Fig. 8, Supplementary Table 1). 27 analysis conducted on zircon cores gave concordant ages ranging from 3015 Ma to 886 Ma (Fig. 7), yielding two major age populations at 912–886 Ma (8 analysis) and 1800–1200 (17 analysis), with the youngest age at 886 ± 11 Ma (Fig. 7, Supplementary Table 1). Among fifty analyses from paragneiss sample 1523–1, seven U–Pb analyses on metamorphic rims yield a concordant weighted average $^{206}Pb/^{238}U$ age of 859 ± 9 Ma (MSWD = 0.59, n = 7) (Fig. 8), with another 19 analysis on metamorphic rims yielding one concordant age of 436 ± 5 Ma and lower intercept ages of 442 ± 52 Ma (MSWD = 15, n = 19)

(Fig. 8, Supplementary Table 1). Ages of 24 zircon cores from this sample range from 2488 Ma to 867 Ma (Fig. 7), yielding two major age populations at 920–867 Ma (6 analysis) and 1800–1200 Ma (12 analysis). The youngest concordant zircon core age is 867 ± 11 Ma. Zircon grains from biotite gneiss sample 1523–2 were mainly selected for zircon core age analysis. Fifty eight analysis in total were conducted, yielding an age range of 2644–851 Ma (Fig. 7, Supplementary Table 1). The youngest core age is dated at 851 ± 11 Ma.

In all, zircon metamorphic rims from the two samples 1523 and 1523-1 yield concordant ages of 860 ± 6 Ma (MSWD=0.37, n=14) and 435 ± 5 Ma (MSWD=0.68, n=5) (Fig. 8), along with lower intercept age of 442 ± 41 Ma (MSWD = 14, n=42). The zircon cores from the three samples yield concordant ages range from 3015 Ma to 851 Ma, with three age populations at 930–865 Ma (22 analysis, peak at 895 Ma), 1850–1200 Ma (52 analysis, peaks at 1480 Ma and 1780 Ma) and a minor age spectra at 2650–2400 Ma (6 analyses, peak at ca. 2500 Ma) (Fig. 10, Supplementary Table 1).

Core-rim structures are mostly absent in detrital zircon grains obtained from the 3 schist samples at Jianning (Fig. 6). The metamorphic rims of the few grains that display core-rim structures are too thin for U–Pb age analysis. Forty analyses were conducted on schist sample 1517, which yield an age range of 2460–736 Ma that display a major age population at 919–736 Ma (32 analysis) (Fig. 9, 10). The youngest concordant grain is dated at 736 ± 15 Ma. Forty six U-Pb age analyses on detrital zircon grains from sample 1519 give an age range of 2942–748 Ma with the youngest grain dated at 748 ± 10 Ma, and yielding a major age population of 840–780

Ma (28 analysis) and a minor one at 2720–2630 Ma (9 analysis) (Fig. 9, 10). Age analysis of 41 detrital zircon grains from sample 1521 range from 2935 Ma to 772 Ma, displaying age populations of 860–770 Ma (19 analysis), 1840–1770 Ma (7 analysis) and 2700–2450 Ma (11 analysis) (Fig. 10). The youngest grain from this sample gives an age of 772 ± 11 Ma (Supplementary Table 1).

In all, the 3 schist samples (1517, 1519 and 1521) from the Jianning area yield three main age populations at 860–736 Ma (73 analysis, peak at 810 Ma), 1835–1775 Ma (10 analysis, peak at 1810 Ma) and 2720–2500 Ma (20 analysis, peak at 2650 Ma) (Fig. 9, 10). The three youngest concordant detrital zircon ages, dated at 748 ± 10, 772 ± 11 and 736 ± 15 Ma, provide a maximum depositional age for the sedimentary protolith of the schist in Jianning area.

5. Discussion

5.1 Age constraints on stratigraphic units and metamorphic events

Our data on detrital zircons from paragneisses and schists of the Wanyuan and Mayuan groups provide constraints on the sedimentation and tectonothermal history of the Cathaysia Block.

The youngest ages determined from detrital zircon cores from the three samples of the Wanyuan Group are 886 ± 11 Ma (sample 1523), 867 ± 11 Ma (sample 1523-1), and 851 ± 11 Ma (sample 1523-2), and these are only slightly older than, or overlap within error, ages for the metamorphic rims of 860 ± 8 Ma (sample 1523) and 859 ± 9 Ma (sample 1523-1). Thus, sedimentation accumulation and subsequent metamorphism were approximately synchronous at around 860 Ma. Conditions of metamorphism at this time are unknown as textural relations between the rim ages and the metamorphic mineral assemblages are not preserved and the other rims within the same samples yield early Paleozoic ages around 440-430 Ma, consistent with ages of the intruded gneissic S-type granite.

Our data from the Mayuan Group indicate it accumulated sometime after ca. 736 Ma on the basis of the youngest detrital zircon grains from the three analyzed samples of 736 ± 15 Ma (sample 1517), 748 ± 10 (sample 1519) and 772 ± 11 (sample 1521), after deposition and ca. 860 Ma metamorphism of the nearby Wanyuan Group.

Mineral assemblages formed during the Neoproterozoic and Paleozoic metamorphism are unknown, as ages of the varying metamorphic grades in Wuyi domain are not precisely constrained. Early Paleozoic strata in the Cathaysia Block are mostly subjected to lower greenschist facies metamorphism. Minor high grade metamorphism reported from Cathaysia occurs in areas adjacent to Paleozoic plutons and is inferred to be associated with their intrusion. Thus, the regional metamorphism that led to formation of Mayuan schist and Wanyuan gneiss most likely occurred in Precambrian time, and the Wanyuan gneiss that contains a metamorphic mineral assemblage of plagioclase, quartz, biotite, hornblende and garnet is suggested to have formed at ca. 860 Ma.

5.2 Tectonic implications

Metamorphism of the Wanyuan Group immediately following its accumulation suggests a tectonic setting adjacent to a convergent plate boundary or during the initial stages associated with a collisional zone setting (Cawood et al., 2012). On the plot of cumulative proportion of analyses vs the difference between crystallization age of the detrital zircons and the depositional age, the Wanyuan Group samples fall either within the convergent margin setting or the transitional field between convergent and collisional settings (Fig. 11; Cawood et al., 2012). In, contrast, the depositional age of the Mayuan Group samples is not well constrained (Fig. 11).

Our data suggest that metamorphism and subduction-collision process likely occurred within the Cathaysia Block at around 860 Ma. Its tectonic location within central Cathaysia, as well as the lower greenschist metamorphism of the Jiangnan belt, suggest that tectonism related to this ca. 860 Ma medium to high grade metamorphism cannot have occurred in the Jiang-Shao suture zone. the presence of this early Neoproterozoic metamorphic event indicates that the Cathaysia Block cannot have been a single unified block at this time. These data also require final assembly of the Cathaysia Block with the Yangtze Block should be younger than ca. 860 Ma, coinciding with convergent plate margin geochemical signature of magmatism from Jiangnan belt throughout ca. 960-830 Ma (Zhao and Cawood 2012; Cawood et al. 2013; Yao et al. 2016). Furthermore, our data for metamorphism of the Wanyuan Group at ca. 860 Ma is the first reliable evidence for Neoproterozoic metamorphism in the Cathaysia Block. Shui (1987) reported a K-Ar age of 844 Ma for amphibolite from rocks ascribed to the Cathaysia Block but the tectonic setting of this location is uncertain and it lies within the Jiang-Shao suture zone. Shui (1987) also reported a metamorphic age of 892 Ma on ultramafic rocks (no method or errors provided) and a K-Ar age of 650 Ma (no errors provided) from schist in the Wuyi domain. Metamorphic zircon from leptite in areas to the southeast of Jianning yield discordant U-Pb $^{206}Pb/^{238}U$ ages of 775–687 Ma and a lower intercept age of 536 ± 1 Ma (Li, 1989). Elsewhere within the South China Craton, 866 ± 14 Ma metamorphic age has been obtained from blueschist in the Jiangnan accretionary belt (Shu et al., 1994), as well as Ar-Ar age of 768 ± 30 Ma on biotite that is inferred to be thrusting related (Hu et al., 1992).

Lithologic, age and geochemical data for early Neoproterozoic rocks units within the Cathaysia Block suggest an accretionary plate margin setting. Mafic igneous rocks ranging in age of 1000–960 Ma display subduction related geochemical signatures (Zhang et al., 2012; Wang et al., 2013). Rhyolite dated at 972 ± 8 Ma and ca. 900 Ma, and 940 Ma amphibolite (Hu and Liu et al., 2002; Shu et al. 2008; Li LM et al., 2011b; Wang et al., 2013) formed in a supra-subduction zone setting, along with 985–913 Ma granitic gneiss occur in various localities of the Cathaysia Block (Wang et al., 2014). These data suggest that the Cathaysia Block is an assemblage of blocks and multiple arcs rather than a unified block during early Neoproterozoic. The ca. 860 Ma metamorphic event documented herein may provide an older age limit on assembly of the block and predates timing of final assembly of the Yangtze and Cathaysia blocks along the Jiangnan orogenic belt, which occurred between ca. 850–800 Ma, possibly within an overall series of convergent plate margin arc systems (Zhao and Cawood, 2012; Cawood et al., 2013; Yao et al., 2014, 2015). The transitional setting from convergent to collisional tectonic setting suggested for the Wanyuan Group on the basis on the zircon data (Fig. 11), suggest the Cathaysia Block was likely part of this overall accretionary assemblage perhaps related to accretion of micro-blocks or arcs. Therefore, previous tectonic models that suggest multiple arc systems within the Cathaysia Block and Jiangnan belt (Cawood et al., 2013; Wang et al., 2013, 2014) and/or divergent double-sided subduction beneath both the Yangtze and Cathaysia blocks (Zhao, 2015) are valid solutions that account for both the age and character of constituent rock units and timing of tectonothermal events.

A second metamorphic event within the study area occurred at 440-430 Ma on the basis of age data from rims on detrital zircons and is suggested to be related to granitic magmatism, also corresponds to the widespread early Paleozoic tectonothermal event that has long been recognized in the Cathaysia Block (Charvet et al., 2010; Shu et al., 2014, 2015 and references therein).

6. Conclusions

Metamorphic ages of ca. 860 Ma and ca. 440 Ma are inferred from paragneiss at Lichuan, with the depositional age of its protolith (Wanyuan Group) constrained at ca. 865–860 Ma, whereas the Mayuan Group from Jianning area accumulated post- ca. 736 Ma. The identified metamorphic ages are indicative of metamorphism and subduction-collision process within the Cathaysia Block at around 860 Ma and suggest it is not a unified block in early Neoproterozoic.

Supplementary Item

Table 1 U–Pb data for detrital zircons from meta-sedimentary rocks in Lichuan and Jianning area, Cathaysia Block can be found in the online version of the Journal at xxxxxxxxxx.

Acknowledgements

Reviews by two anonymous reviewers are gratefully acknowledged for their constructive comments and suggestions that led to a major improvement of the manuscript. We also thank Dr. J.Q. Wang for his help with zircon dating. We acknowledge the financial support by the Major State Research Development Program of China (Grant No. 2016YFC0600202), National Natural Science Foundation of China (Nos. 41330208 and 41572200) and State Key Laboratory for Mineral Deposits Research (Nanjing University) (ZZKT-201603).

References

1. BGMRFJ (Bureau of Geology and Mineral Resources of Fujian Province), 1985. Regional Geology of Fujian Province. Geological Publishing House, Beijing, pp. 7–564 (in Chinese with English abstract).

2. BGMRJX (Bureau of Geology and Mineral Resources of Jiangxi Province), 1984. Regional Geology of Guangxi Autonomous Region. Geol. Publ. House, Beijing, P. 1–921 (In Chinese with English Abstract).

3. Cawood, P.A., Hawkesworth, C.J., Dhuime, B., 2012. Detrital zircon record and tectonic setting. Geology 40 (10), 875–878.

4. Cawood, P.A., Wang, Y.J., Xu, Y.J., Zhao, G.C., 2013. Locating South China in Rodinia and Gondwana: a fragment of Greater Indian Lithosphere? Geology 41(8), 903–906.

5. Charvet, J., Shu, L.S., Faure, M., Choulet, F., Wang, B., Lu, H.F., Le Breton, N., 2010. Structural development of the Lower Paleozoic belt of South China: Genesis of an intracontinental orogen. Journal of Asian Earth Sciences 39, 309–330.

6. Chen, C.H., Lee, C.Y., Hsieh, P.S., Zeng, W., Zhou, H.W., 2008. Approaching the Age Problem for Some Metamorphosed Precambrian Basement Rocks and Phanerozoic Granitic Bodies in the Wuyishan Area: The Application of EMP Monazite Age Dating. Geological Journal of China Universities 14(1), 1-15.

7. Corfu, F., Hanchar, J.M., Hoskin, P.W.O., Kinny, P., 2003. Altas of zircon textures. Reviews in Mineralogy and Geochemistry 53, 469–500

8. Harley, S.L., Kelly, N.M., Möller, A., 2007. Zircon behaviour and the thermal histories of mountain chains. Elements 3, 25–30.

9. Hu, G.R., Liu, C.Q., 2002. Geochemistry of amphibolites from the Zhoutan group, Jiangxi Province: implications for the tectonic settings. Acta Mineralogica Sinica 22 (4), 336–342.

10. Jiang, Y.H., Wang, G.C., Liu, Z., Ni, C.Y., Qing, L., Zhang, Q., 2015. Repeated slab advance–retreat of the Palaeo-Pacific plate underneath SE China. International Geology Review 57(4), 472–491.

11. Li, G. K., 1989, Isotopic ages of the basement rocks in Fujian Province and their implications for regional tectonic evolution. Fujian Geology 8, 159–168 (in Chinese).

12. Li, X.H., 1997. Timing of the Cathaysia block formation: constraints from SHRIMP U–Pb zircon geochronology. Episodes 20, 188–192

13. Li, L.M., Sun, M., Wang, Y.J., Xing, G.F., Zhao, G.C., Cai, K.D., Zhang, Y.Z., 2011a. Geochronology and geochemistry of Palaeoproterozoic gneissic granites and clinopyroxenite enclaves from NW Fujian, SE China: implications for the crustal evolution of the Cathaysia Block. Journal of Asian Earth Science 41, 204–212.

14. Li, L.M., Sun, M., Wang Y.J., Xing, G.F., Zhao, G.C., Lin, S.F., Xia, X.P., Chan, L.S., Zhang, F.F., Wong, J., 2011b. U-Pb and Hf isotopic study of zircons from migmatised amphibolites in the Cathaysia Block: Implications for the early Paleozoic peak tectonothermal event in Southeastern China. Gondwana Research 19, 191–201.

15. Ludwig, K.R., 2003. Isoplot 3.00, a geochronological Toolkit for Microsoft Excel. Berkeley Geochronology Center, Special Publication 4, 1-70.

16. Shu, L. S., Zhou, G. Q., Shi, Y. S., Yin, J., 1994. Study on the high pressure metamorphic blueschist and its late Proterozoic age in the eastern Jiangnan belt. Chinese Science Bulletin 39, 1200–1204.

17. Shu, L.S., 2006. Predevonian Tectonic Evolution of South China: from Cathaysian Block to Caledonian Period Folded Orogenic Belt. Geological Journal of China Universities 12(4), 418-431 (In Chinese with English abstract).

18. Shu, L.S., Deng, P., Yu, J.H., Wang, Y.B., Jiang, S.Y., 2008. The age and tectonic environment of the rhyolitic rocks on the western side of Wuyi Mountain, South China. Science in China (series D) 51 (8), 1053–1063.

19. Shu, L.S., Faure, M., Yu, J.H., Jahn, B.M., 2011. Geochronological and geochemical features of the Cathaysia Block (South China): New evidence for the Neoproterozoic breakup of Rodinia. Precambrian Research 187 (3–4), 263–276.

20. Shu, L.S., 2012. An analysis of principal features of tectonic evolution in South China Block. Geological Bulletin of China 31(7), 1035-1053.

21. Shu, L.S., Jahn, B.M., Charvet, J., Santosh, M., Wang, B., Xu, X.S., and Jiang, S.Y., 2014. Early Paleozoic depositional environment and intracontinental orogeny in the Cathaysia Block (South China): implications from stratigraphic, structural, geochemical and geochronologic evidence. American Journal of Science 314, 154-186.

22. Shu, L., Wang, B., Cawood, P. A., Santosh, M., Xu, Z.Q., 2015. Early Paleozoic and early Mesozoic intraplate tectonic and magmatic events in the Cathaysia Block, South China. Tectonics 34, 1600-1621.

23. Shui, T., 1987, Tectonic framework of the southeastern China continental basement: Scientia Sinica B30, 414–422 (in Chinese).

24. Song, M.J., Shu, L.S., Santosh, M., Li, J.Y., 2015. Late Early Paleozoic and Early Mesozoic intracontinental orogeny in the South China Craton: Geochronological and geochemical

evidence. Lithos 232, 360-374.

25. Vavra, G., Schmidt, R., Gebauer, D., 1999. Internal morphology, habit and U–Th–Pb microanalysis of amphibolite-to-granulite facies zircons: geochronology of the Ivrea Zone (Southern Alps). Contributions to Mineralogy and Petrology 134, 380–404.

26. Wan, Y.S., Liu, D.Y., Xu, M.H., Zhuang, J.M., Song, B., Shi, Y.R., Du, L.L., 2007. SHRIMP U–Pb zircon geochronology and geochemistry of metavolcanic and metasedimentary rocks in Northwestern Fujian, Cathaysia block, China: Tectonic implications and the need to redefine lithostratigraphic units. Gondwana Research 12, 166–183.

27. Wang, Y.J., Zhang, A.M., Cawood, P.A., Fan, W.M., Xu, J.F., Zhang, G.W., Zhang, Y.Z., 2013. Geochronological, geochemical and Nd-Hf-Os isotopic fingerprinting of an early Neoproterozoic arc-back-arc system in South China and its accretionary assembly along the margin of Rodinia. Precambrian Research 231, 343–371.

28. Wang, Y.J., Zhang, Y.Z., Fan, W.M., Geng, H.Y., Zou, H.P., Bi, X.W., 2014. Early Neoproterozoic accretionary assemblage in the Cathaysia block: geochronological, Lu–Hf isotopic and geochemical evidence from granitoid gneisses. Precambrian Research 249, 144–161.

29. Yu, J.H., Zhou, X.M., Zhao, L., 2003. Discovery and implications of granulite facies metamorphic rocks in the eastern Nanling, China. Acta Petrologica Sinica 19 (3), 461–467 (in Chinese with English abstract).

30. Yu, J.H., Zhou, X.M., O'Reilly, S.Y., 2005. Formation history and protolith characteristics of granulite facies metamorphic rock in Central Cathaysia deduced from U–Pb and Lu–Hf isotopic studies of single zircon grains. Chinese Science Bulletin 50 (18), 2080–2089.

31. Yao, J.L, Shu, L.S., Santosh, M., Zhao, G.C., 2014. Neoproterozoic arc-related mafic-ultramafic rocks and syn-collision granite from the western segment of the Jiangnan Orogen, South China: constraints on the Neoproterozoic assembly of the Yangtze and Cathaysia Blocks. Precambrian Research 243, 39– 62.

32. Yao, J.L., Shu, L.S., Santosh, M., Li, J.Y., 2015. Neoproterozoic arc-related andesite and orogeny-related unconformity in the eastern Jiangnan orogenic belt: Constraints on the assembly of the Yangtze and Cathaysia blocks in South China. Precambrian Research 262, 84–100.

33. Yao, J.L., Cawood, P.A., Shu, L.S., Santosh, M., Li, J.Y., 2016. An Early Neoproterozoic Accretionary Prism Ophiolitic Mélange from the Western Jiangnan Orogenic Belt, South China. The Journal of Geology 124, 587–601.

34. Zhang, A.M., Wang, Y.J., Fan, W.M., Zhang, Y.Z., Yang, J., 2012. Earliest Neoproterozoic (ca. 1.0 Ga) arc–back-arc-basin nature along the northern Yunkai Domain of the Cathaysia Block: geochronological and geochemical evidence from the metabasite. Precambrian Research 220-221, 217–233.

35. Zhang, Y., Shu, L.S., Chen, X.Y., 2011. Study of geochemistry, geochronology and petrogenesis of the Early Paleozoic granitic plutons in the central–southern Jiangxi Province. Science in China (Earth Sciences) 54, 1492–1510.

36. Zhao, G.C., 2015. Jiangnan Orogen in South China: Developing from divergent double subduction. Gondwana Research 27(3), 1173–1180.

37. Zhao, G.C., Cawood, P.A., 1999. Tectonothermal evolution of the Mayuan assemblage in the Cathaysia Block: new evidence for Neoproterozoic collisional-related assembly of the South

China craton. American Journal of Science 299, 309–339.

38. Zhao, G.C., Cawood, P.A., 2012. Precambrian geology of China. Precambrian Research 222–223, 13–54.

Captions of figures

Fig.1. Geological sketch map of the Cathaysia Block, South China Craton (1: Jiangshan-Shaoxing fault; 2: Zhenghe-Dapu fault; 3: Northeast Jiangxi fault; 4: Jiujiang-Shitai fault; 5: Tanlu fault; SECCLMVZ: Southeast China costal late Mesozoic volcanic zone; SJX-NL: southern Jiangxi - Nanling).

Fig.2. Geological sketch map of the Cathaysia Block at Lichuan and Jianning area, South China.

Fig.3. (a) Cross section with sample locations of Lichuan region; (b) Cross section with sample locations of Jianning region.

Fig.4. Representative field photos of samples analyzed in this study. (A) and (B) Field photograph of the Biotite quarts schist sample 1517; (C) and (D) Field photograph showing the location of kyanite schist sample 1521; (E) Field photograph showing the location of migmatized paragneiss; (F) Field photograph of the biotite gneiss sample 1523; (G) Field photograph of the biotite gneiss sample 1523-1; (H) Field photograph of migmatite.

Fig.5. Photomicrographs of samples analyzed in this study. (A) Thin section

photomicrograph of kyanite schist sample 1517 (plane-polarized light); (B) Thin section photomicrograph of sample 1519 (crossed nicols); (C) Photomicrograph of sample 1521 (crossed nicols); (D) Thin section photomicrograph of sample 1523 (plane-polarized light); (E) Photomicrograph of sample 1523-1 (plane-polarized light); (F) Photomicrograph of migmatized schist sample 1523-2 (crossed nicols). (Qz, quartz; Mus, Muscovite; Bt, Biotite; Plag, plagioclase; HB, hornblende; Grt, Garnet; Ky, kyanite)

Fig. 6. Reprehensive CL images of detrital zircons from meta-sedimentary rocks in Lichuan and Jianning area.

Fig.7. U–Pb concordia plots for detrital zircons from paragneiss of Wanyuan Group in Lichuan region;

Fig. 8. U-Pb concordia plots for metamorphic rims of detrital zircon from paragneiss from Wanyuan Group in Lichuan region.

Fig. 9. U-Pb concordia plots for detrital zircons from schist of Mayuan Group in Jianning region.

Fig.10. A: U–Pb age probability density plot for detrital zircons from schist in Jianning area and paragneisses in Lichuan area.

Fig. 11. Plot of cumulative proportions vs. CA–DA (CA: crystallization ages and DA: depositional age) of analyzed detrital zircons (after Cawood et al., 2012). (A: convergent setting; B: collisional setting; C: extensional setting).

Captions of tables

Table 1 U–Pb data for detrital zircons from meta-sedimentary rocks in Lichuan and Jianning area, Cathaysia Block.

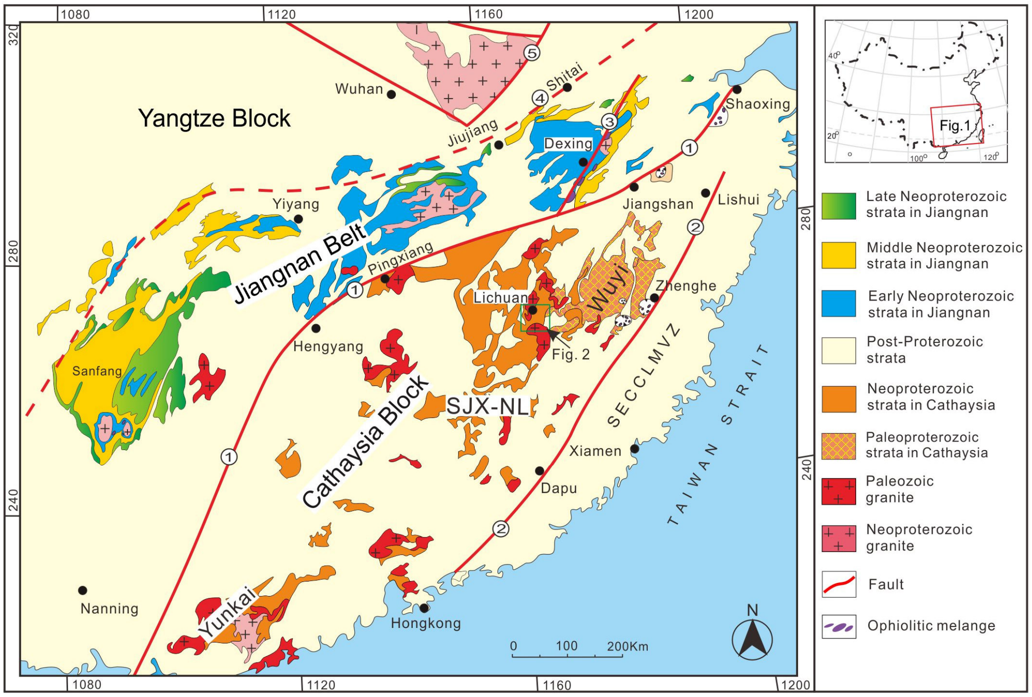

Yangtze Block
Wuhan
Shitai
Shaoxing
Jiujiang
Dexing
Yiyang
Jiangshan
Lishui
Jiangnan Belt
Pingxiang
Lichuan
Wuyi
Zhenghe
Hengyang
Fig. 2
Sanfang
SJX-NL
Cathaysia Block
SECCLMVZ
TAIWAN STRAIT
Xiamen
Dapu
Yunkai
Hongkong
Nanning
0 100 200Km
N
Fig.1
Late Neoproterozoic strata in Jiangnan
Middle Neoproterozoic strata in Jiangnan
Early Neoproterozoic strata in Jiangnan
Post-Proterozoic strata
Neoproterozoic strata in Cathaysia
Paleoproterozoic strata in Cathaysia
Paleozoic granite
Neoproterozoic granite
Fault
Ophiolitic melange

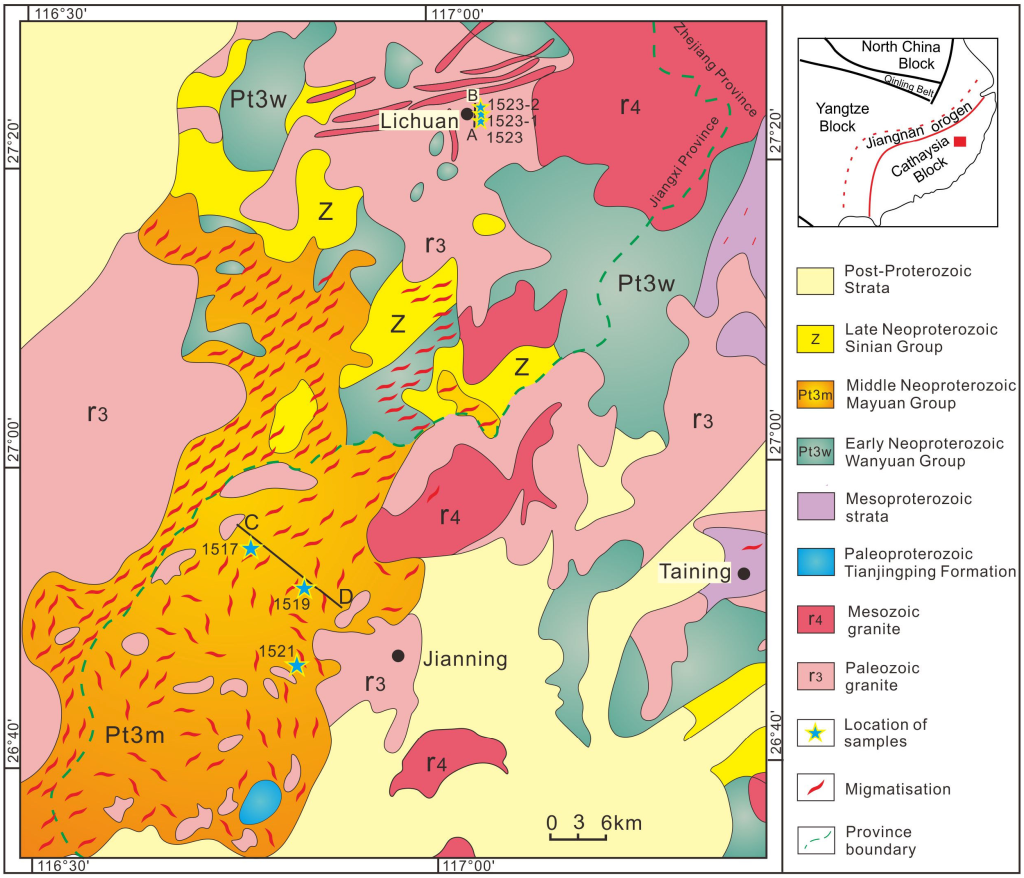

116°30'
117°00'
27°20'
27°00'
26°40'
Pt3w
Lichuan
B
A
1523-2
1523-1
1523
r4
Zhejiang Province
Jiangxi Province
Z
r3
Pt3w
Z
Z
r3
r3
C
1517
1519
D
r4
Taining
1521
Jianning
r3
Pt3m
r4
0 3 6km
North China Block
Qinling Belt
Yangtze Block
Jiangnan orogen
Cathaysia Block
Post-Proterozoic Strata
Late Neoproterozoic Sinian Group
Middle Neoproterozoic Mayuan Group
Early Neoproterozoic Wanyuan Group
Mesoproterozoic strata
Paleoproterozoic Tianjingping Formation
Mesozoic granite
Paleozoic granite
Location of samples
Migmatisation
Province boundary

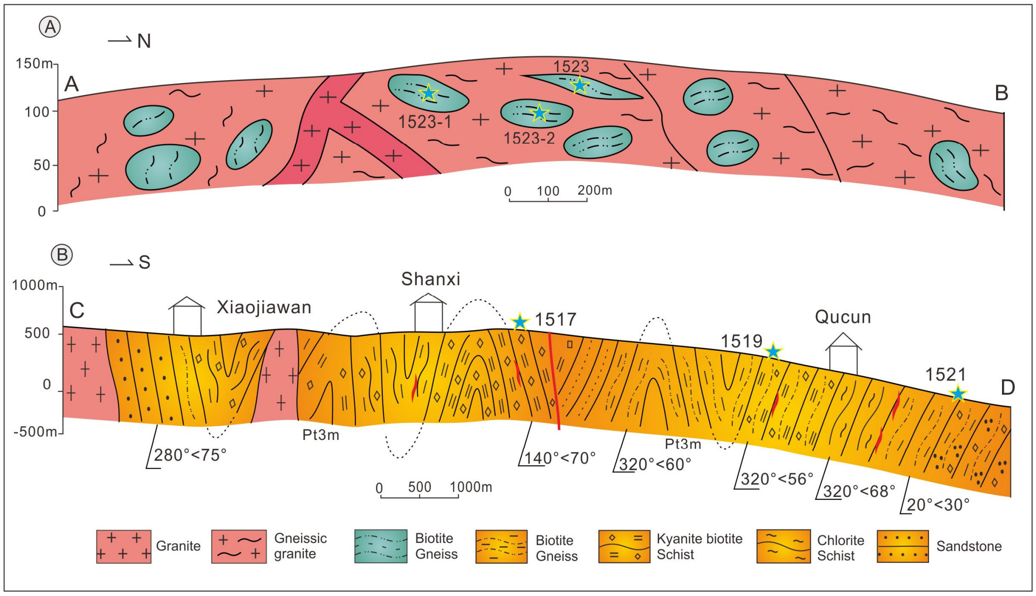
A
N
150m
100
50
0
A
B
1523
1523-1
1523-2
0 100 200m
B
S
1000m
500
0
-500m
C
D
Xiaojiawan
Shanxi
Qucun
1517
1519
1521
Pt3m
Pt3m
280°<75°
140°<70°
320°<60°
320°<56°
320°<68°
20°<30°
0 500 1000m
Granite
Gneissic granite
Biotite Gneiss
Biotite Gneiss
Kyanite biotite Schist
Chlorite Schist
Sandstone

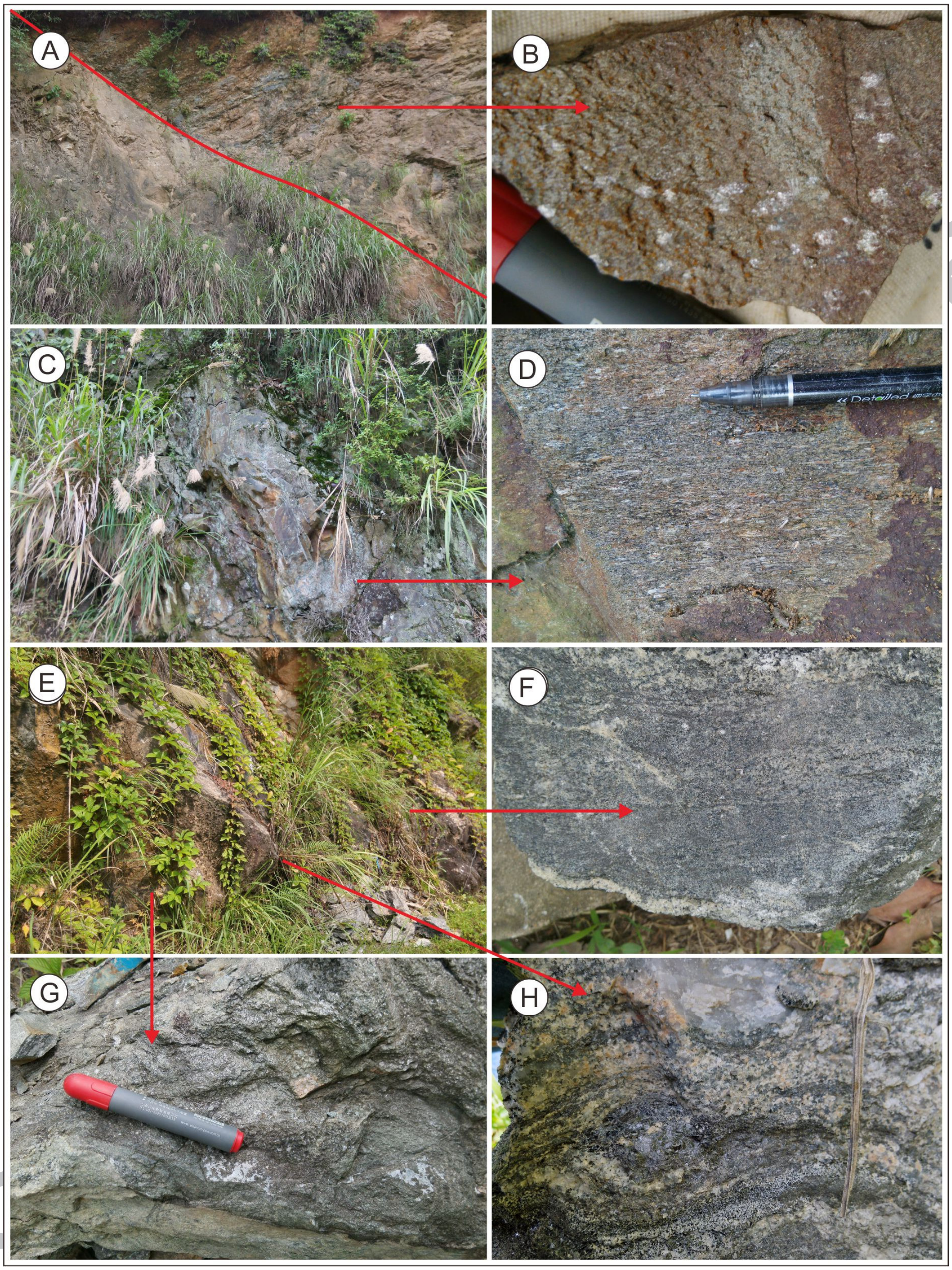
A
B
C
D
E
F
G
H

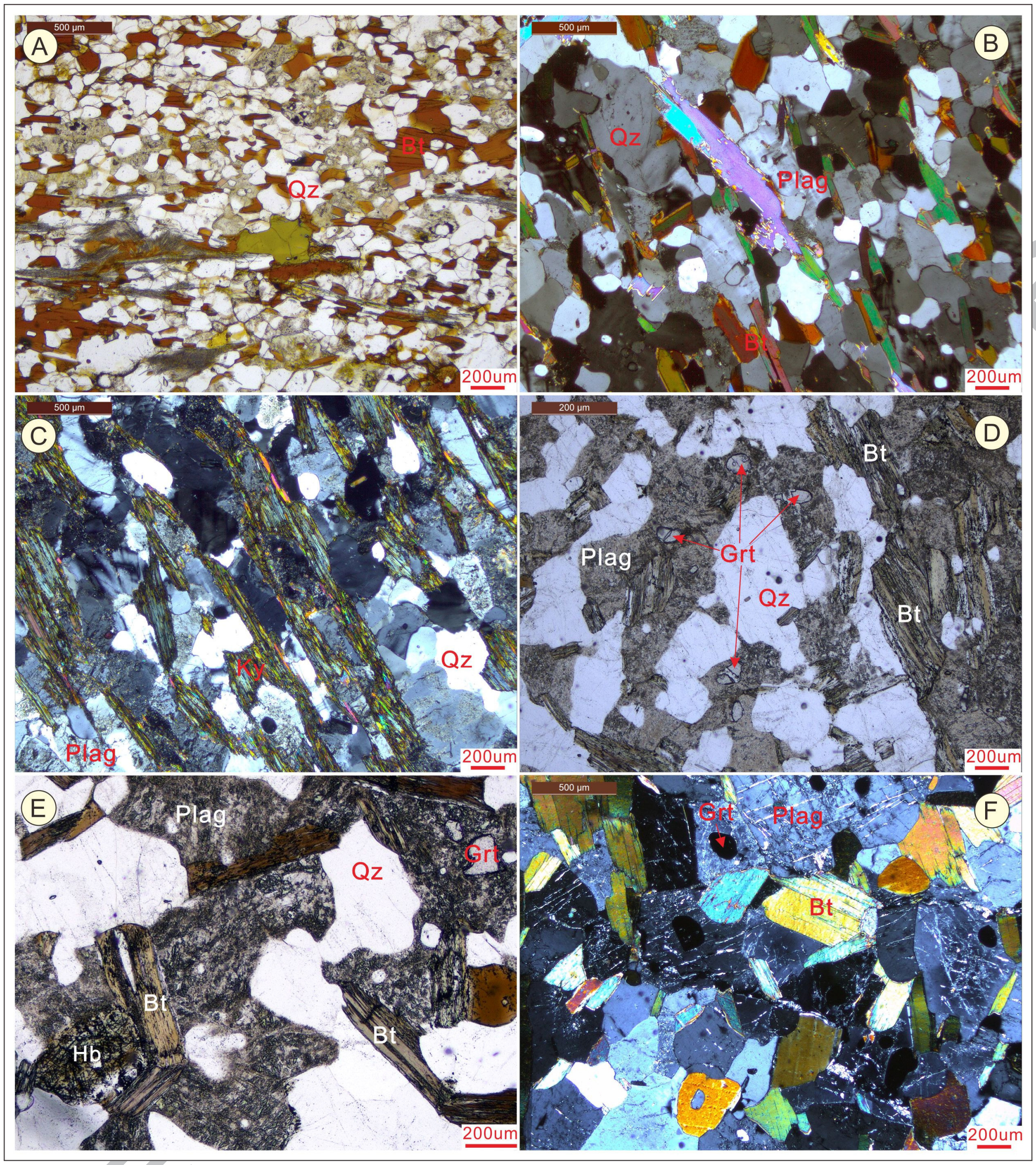

A
500 µm
Bt
Qz
200um
B
500 µm
Qz
Plag
Bt
200um
C
500 µm
Ky
Qz
Plag
200um
D
200 µm
Bt
Plag
Grt
Qz
Bt
200um
E
Plag
Grt
Qz
Bt
Hb
Bt
200um
F
500 µm
Grt
Plag
Bt
200um

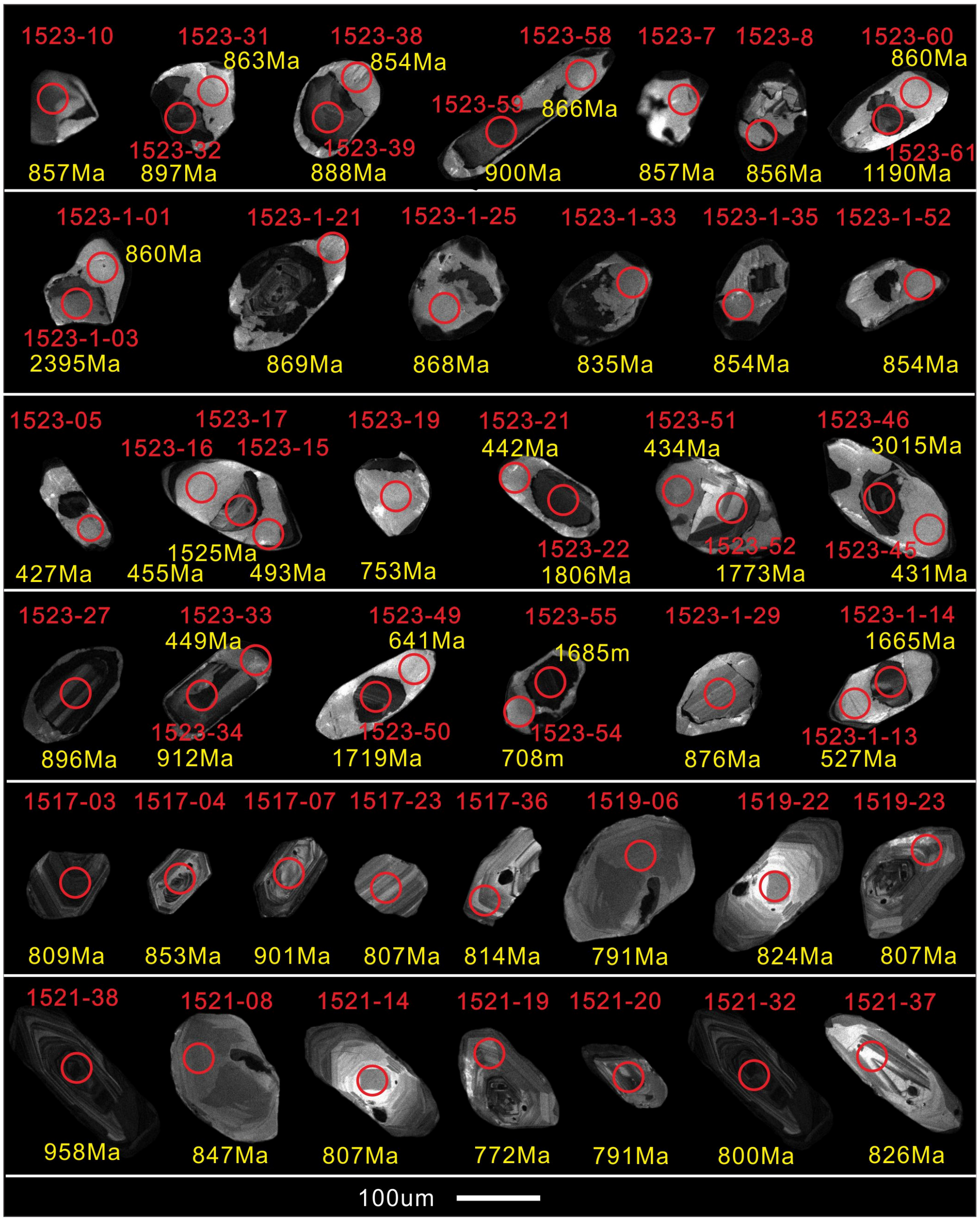

1523-10
857Ma
1523-31
863Ma
1523-32
897Ma
1523-38
854Ma
1523-39
888Ma
1523-58
866Ma
1523-59
900Ma
1523-7
857Ma
1523-8
856Ma
1523-60
860Ma
1523-61
1190Ma
1523-1-01
860Ma
1523-1-03
2395Ma
1523-1-21
869Ma
1523-1-25
868Ma
1523-1-33
835Ma
1523-1-35
854Ma
1523-1-52
854Ma
1523-05
427Ma
1523-17
1523-16
1523-15
1525Ma
455Ma
493Ma
1523-19
753Ma
1523-21
442Ma
1523-22
1806Ma
1523-51
434Ma
1523-52
1773Ma
1523-46
3015Ma
1523-45
431Ma
1523-27
896Ma
1523-33
449Ma
1523-34
912Ma
1523-49
641Ma
1523-50
1719Ma
1523-55
1685m
1523-54
708m
1523-1-29
876Ma
1523-1-14
1665Ma
1523-1-13
527Ma
1517-03
809Ma
1517-04
853Ma
1517-07
901Ma
1517-23
807Ma
1517-36
814Ma
1519-06
791Ma
1519-22
824Ma
1519-23
807Ma
1521-38
958Ma
1521-08
847Ma
1521-14
807Ma
1521-19
772Ma
1521-20
791Ma
1521-32
800Ma
1521-37
826Ma
100um

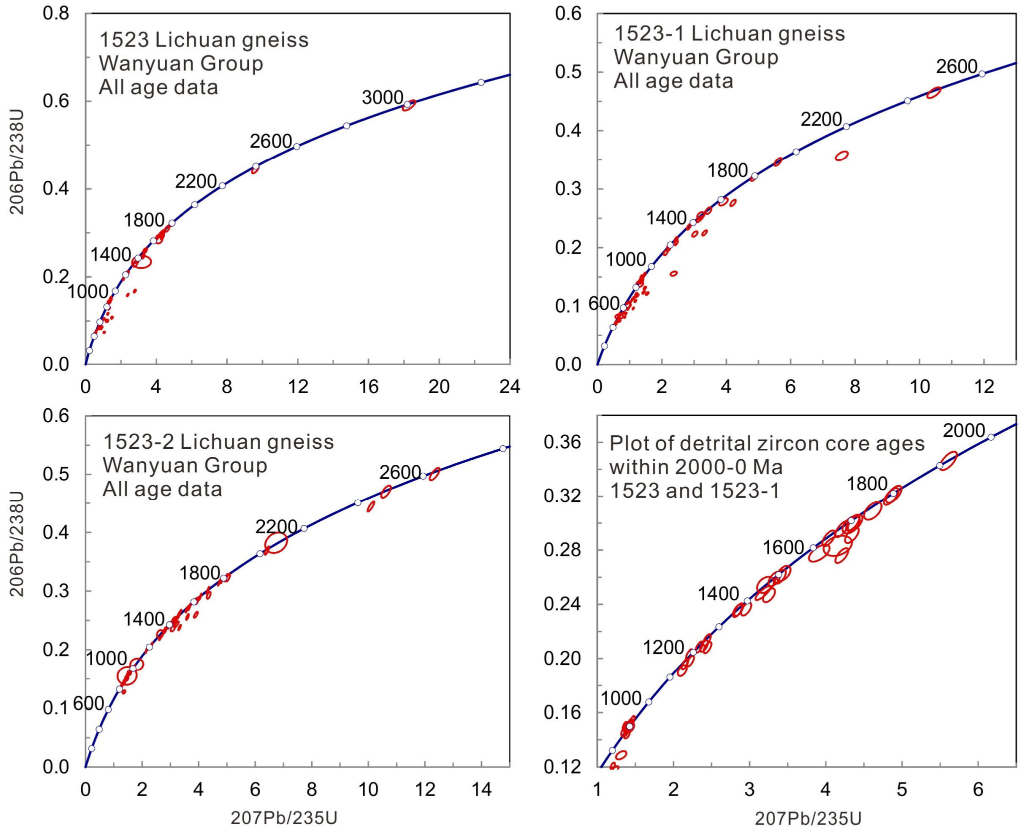
1523 Lichuan gneiss
Wanyuan Group
All age data
1523-1 Lichuan gneiss
Wanyuan Group
All age data
1523-2 Lichuan gneiss
Wanyuan Group
All age data
Plot of detrital zircon core ages
within 2000-0 Ma
1523 and 1523-1
206Pb/238U
207Pb/235U
3000
2600
2200
1800
1400
1000
600
1600
1200
2000

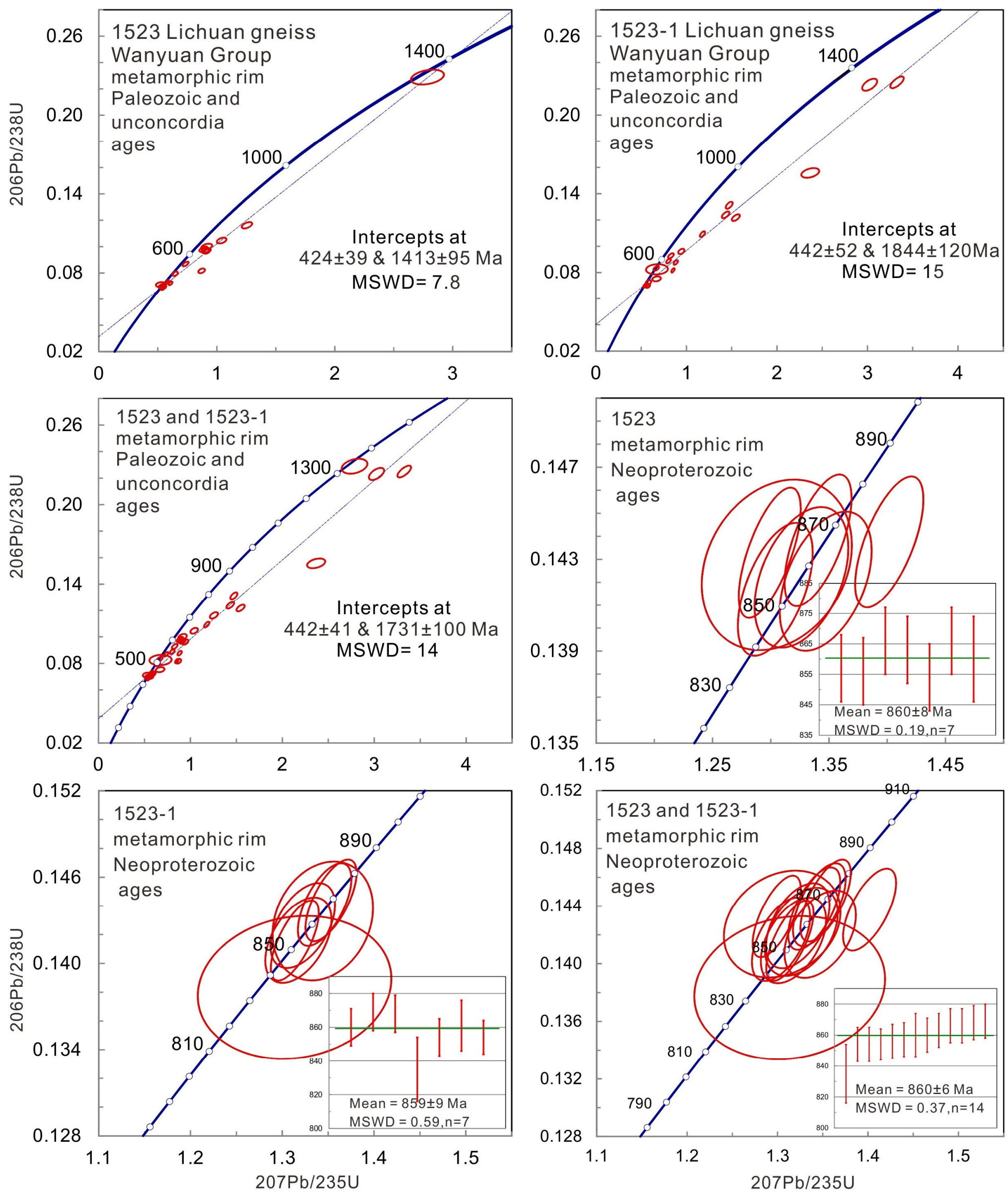

1523 Lichuan gneiss
Wanyuan Group
metamorphic rim
Paleozoic and
unconcordia
ages
Intercepts at
424±39 & 1413±95 Ma
MSWD= 7.8
1523-1 Lichuan gneiss
Wanyuan Group
metamorphic rim
Paleozoic and
unconcordia
ages
Intercepts at
442±52 & 1844±120Ma
MSWD= 15
1523 and 1523-1
metamorphic rim
Paleozoic and
unconcordia
ages
Intercepts at
442±41 & 1731±100 Ma
MSWD= 14
1523
metamorphic rim
Neoproterozoic
ages
Mean = 860±8 Ma
MSWD = 0.19,n=7
1523-1
metamorphic rim
Neoproterozoic
ages
Mean = 859±9 Ma
MSWD = 0.59,n=7
1523 and 1523-1
metamorphic rim
Neoproterozoic
ages
Mean = 860±6 Ma
MSWD = 0.37,n=14
206Pb/238U
207Pb/235U

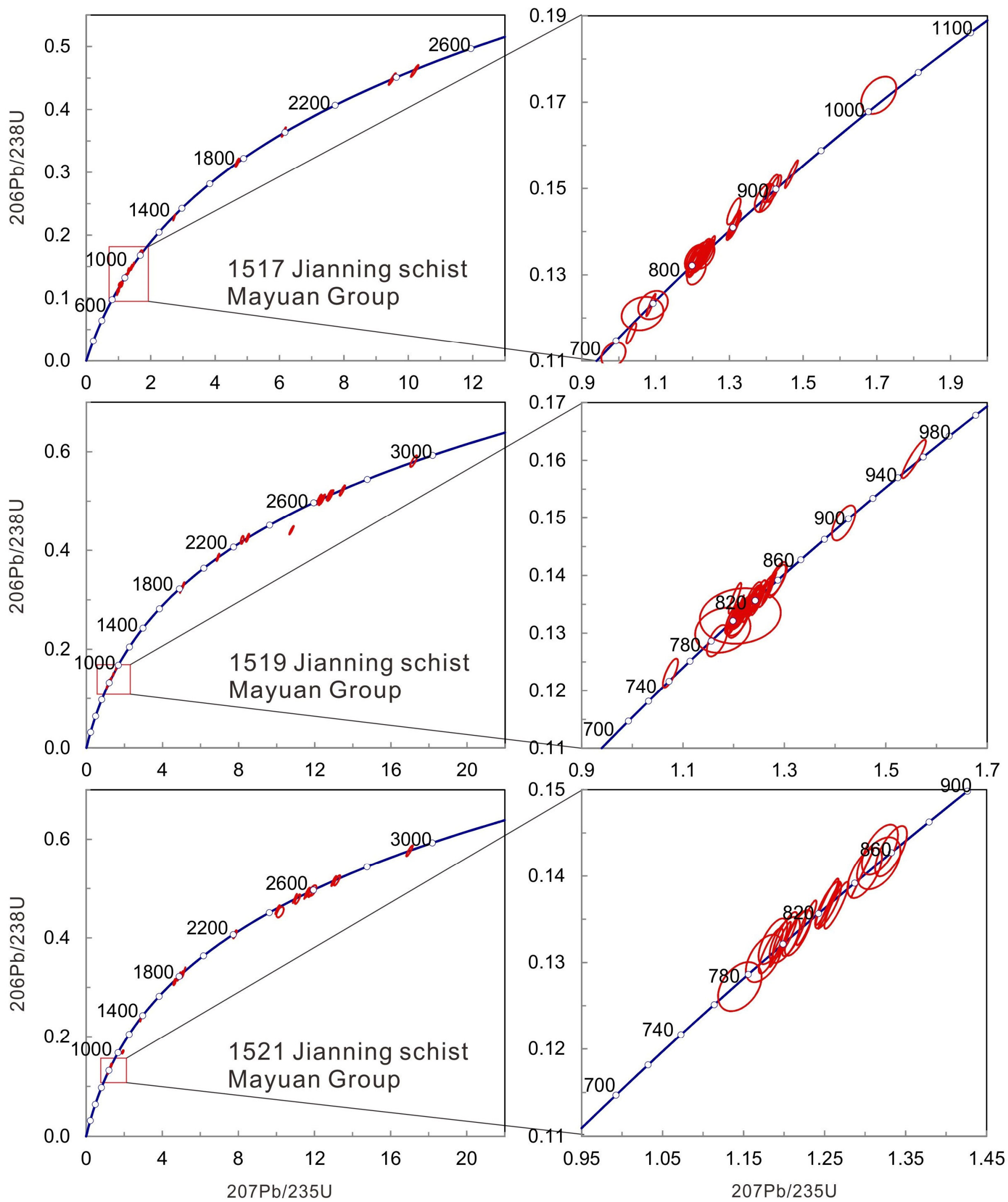

1517 Jianning schist
Mayuan Group
1519 Jianning schist
Mayuan Group
1521 Jianning schist
Mayuan Group
206Pb/238U
207Pb/235U

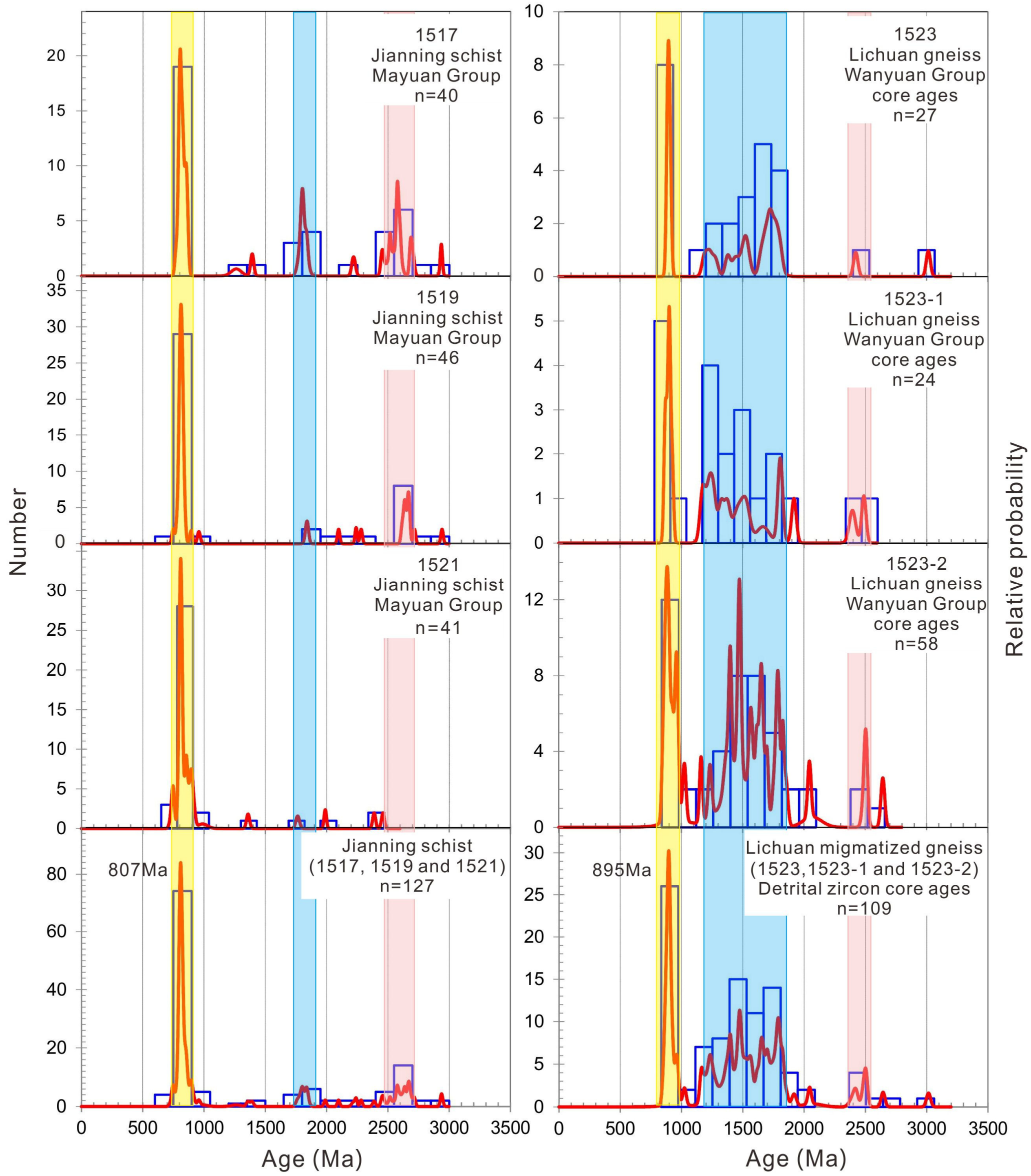

1517
Jianning schist
Mayuan Group
n=40
1519
Jianning schist
Mayuan Group
n=46
1521
Jianning schist
Mayuan Group
n=41
807Ma
Jianning schist
(1517, 1519 and 1521)
n=127
1523
Lichuan gneiss
Wanyuan Group
core ages
n=27
1523-1
Lichuan gneiss
Wanyuan Group
core ages
n=24
1523-2
Lichuan gneiss
Wanyuan Group
core ages
n=58
895Ma
Lichuan migmatized gneiss
(1523,1523-1 and 1523-2)
Detrital zircon core ages
n=109
Number
Relative probability
Age (Ma)
Age (Ma)

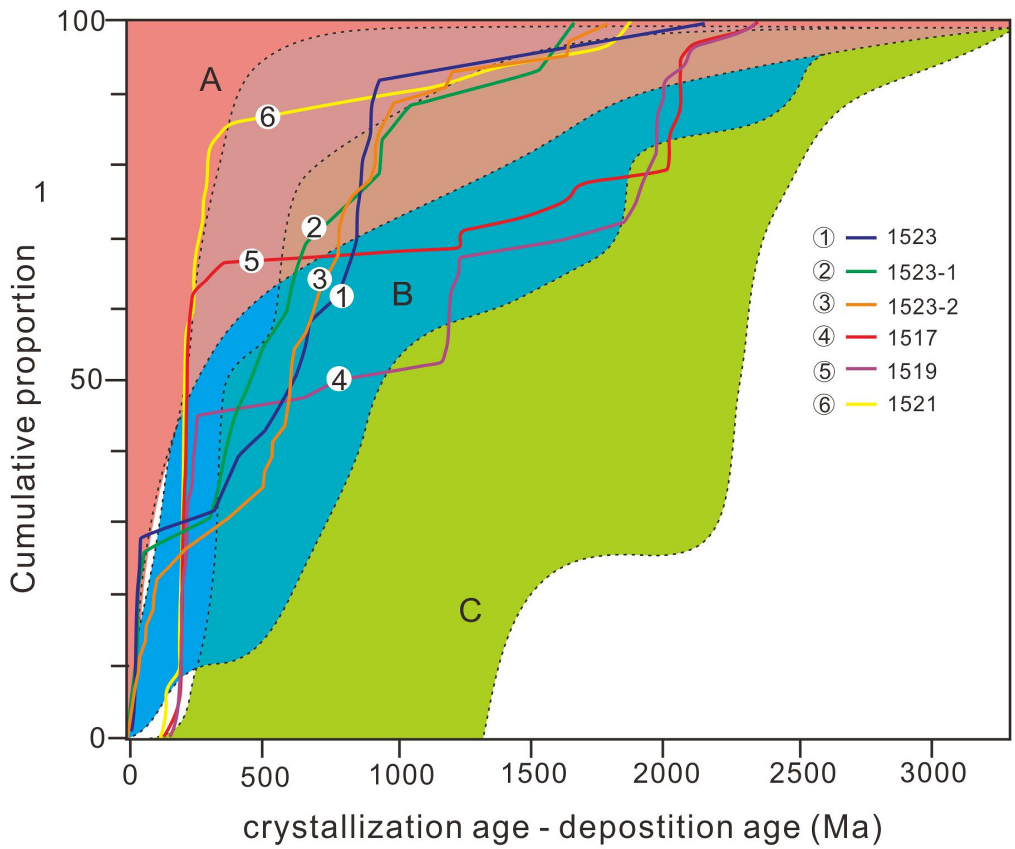
100
50
0
1
Cumulative proportion
0
500
1000
1500
2000
2500
3000
crystallization age - depostition age (Ma)
A
B
C
① 1523
② 1523-1
③ 1523-2
④ 1517
⑤ 1519
⑥ 1521

Research highlights

- Evidence of metamorphism at ca. 860 Ma obtained from the Cathaysia Block
- The Cathaysia Block was not a unified block in early Neoproterozoic